Effect of Zinc Acetate Dihydrate Concentration on the Characteristics of Electrospun PVA Coatings on Magnesium Implants

Bambang Suharno[1], Sugeng Supriadi[2*], Andi Ridzky Widarto[1], and Amirah Salsabila Widad Putri[2]

[1]Department of Metallurgical & Materials Engineering, Faculty of Engineering, Universitas Indonesia, Depok, Indonesia
[2]Department of Mechanical Engineering, Faculty of Engineering, Universitas Indonesia, Depok, Indonesia
*Correspondence: sugeng@eng.ui.ac.id

Abstract. This study investigates the impact of varying concentrations of zinc acetate dihydrate on the morphological and surface properties of electrospun polyvinyl alcohol (PVA) fiber layers applied to magnesium substrates, intended for use as a biodegradable implant material. Electrospinning was employed to fabricate PVA/ZnAc composite fiber layers by incorporating different ZnAc concentrations into PVA solutions. The researcher focuses on evaluating key parameters of the resulting fiber layers, including fiber diameter, layer thickness, porosity, and surface wettability, as determined by contact angle measurements. The experimental results demonstrate that increasing the concentration of zinc acetate dihydrate leads to a noticeable enlargement in fiber diameter and a corresponding increase in both the overall thickness and porosity of the electrospun layers. Specifically, the fiber layer at 50% ZnAc concentration exhibited the highest thickness of 0.0108 mm, while also producing the largest average fiber diameter of 2.162 nm ± 0.86 nm. Additionally, higher ZnAc concentrations were found to enhance the hydrophobic nature of the coatings, as indicated by higher contact angle values. Among all samples, the 20% ZnAc concentration demonstrated superhydrophilic behavior with the lowest contact angle value of 44.76° ± 1.84°. However, this increase in hydrophobicity is also associated with an undesirable rise in the corrosion rate of the magnesium substrate, suggesting a trade-off between surface modification and material stability. These findings highlight the importance of optimizing ZnAc content in PVA solutions to achieve a balance between desired fiber morphology and corrosion resistance. Ultimately, the study underscores that careful selection of zinc acetate dihydrate concentration is vital for developing functional and reliable electrospun PVA/ZnAc coatings for magnesium-based biodegradable implants.

Keywords: Magnesium implants, Coating, Electrospinning, Polyvinyl alcohol, Acetate dihydrate.

S. C. Asih et al. (eds.), *Proceedings of the 19th International Conference on Quality in Research (QiR 2025)*, Advances in Engineering Research 303,
https://doi.org/10.2991/978-94-6239-717-0_23

1 Introduction

Biomaterials are materials that interact directly with the body's biological tissues and fluids and function to treat, repair or replace body parts. Biomaterials are used to replace or improve the function of tissue and/or organs that have been damaged or degenerated due to aging, so that the patient's quality of life can improve. The properties of biomaterials used as regenerative medicine depend on the nature of the material from which they are made (polymer, ceramic, metal, or composite), their shape (solid material, porous material), and their spatial construction (physical properties, chemical properties) [1, 2]. Biomaterials must have properties that make them capable of carrying out their function well, both as implants and as medical devices. Several characteristics that biomaterials as implants must have include: 1) elastic modulus close to real bone (18 GPa), mechanical strength, wettability, surface roughness and good corrosion resistance [3]. Degradable materials have been used in medicine for decades. The basic concept in biodegradable implants is that they are composed of elements that can be eliminated from the body through physiological pathways and do not exceed toxicity limits during the degradation process [2, 4]. Currently, the application of biomaterials for bone implants only pays attention to high strength and toughness specifications. In this case, metallic biomaterials are often the choice in clinical applications. Some metal materials commonly used in the medical world today include titanium-based alloys, magnesium, and many more [5, 6].

Magnesium (Mg) is receiving special attention in the current development of biomaterial science due to its good mechanical ability and biocompatibility as a biomaterial. The use of Mg as a bone implant biomaterial is not only because the mechanical strength of Mg is close to the strength of real bone, but also because Mg can decay in the environmental conditions of the human body and can be excreted biologically through urine [7]. The toughness of Mg is greater than ceramic biomaterials such as hydroxyapatite, with an elastic modulus value that is close to the human elastic modulus of 45 GPa, so it can reduce the possibility of stress shielding and loss of bone density and strength [8]. Besides, Mg is very good for the human body because Mg2+ ions are needed in large quantities for metabolic reactions and biological mechanisms [9, 10].

Even though all the optimization methods given above can increase the corrosion resistance of Mg materials, it is still difficult to achieve the desired biocompatibility as an implant. That is one of the reasons research on surface modification is a topic of increasing interest in magnesium as a biomedical material [11]. It’s possible to carry out surface modifications to improve the quality of the magnesium material [12]. This method is economically cheaper and widely used. One surface modification method option that can be used is electrospinning. Electrospinning is a fiber-forming process with electrostatic forces to control fiber formation [13]. One of the polymers that is popularly used in many medical applications is poly(vinyl) alcohol (PVA) because of its flexibility to be used in various applications and the ease of PVA to be processed and used in various processing technologies [14, 15]. PVA is a type of polymer with non-toxic, biocompatible properties and good chemical and thermal stability. PVA also has supporting properties such as solubility, viscosity, surface tension, and molecular weight which are suitable as electrospinning materials to produce nanofibers [16, 17].

However, despite its versatility, electrospinning still faces inherent limitations that restrict its broader application for implants. The technique is highly sensitive to ambient conditions, where variations in relative humidity and temperature can lead to jet instabilities, bead formation, fiber fusion, or uncontrolled diameter changes. This sensitivity often results in poor reproducibility and significant batch-to-batch variability, which becomes problematic in clinical applications requiring standardized implant quality [18-20]. In addition, scaling up electrospinning remains a challenge because of the complex interplay between solution properties, processing parameters,

and environmental factors. Producing large-area, multilayered, or thick fiber constructs consistently is technically difficult, and industrial-scale electrospinning systems (such as multi-jet setups) often introduce further variability [21, 22]. These limitations highlight this work as the need for careful parameter optimization and innovation in process control to ensure electrospinning can reliably support biomedical implant development.

2 Materials and Methods

2.1 Materials

The polymer solution was obtained by dissolving Poly(vinyl)alcohol powder (PVA, Merck, Mw = 72,000) with distilled water with a weight ratio (g) of 1:10 using a magnetic stirrer for 4 hours, then dissolving the Zinc Acetate dihydrate (CH3COO)2Zn*2H2O powder Merck with distilled water with a weight ratio (g) of 1: 5 using a magnetic stirrer for 2 hours. The PVA solution and ZnAc solution were mixed and stirred for 4 hours with varying ZnAc concentrations of 20%, 25%, 33%, 50%.

2.2 Methods

Sample is prepared through polishing and etching. Sample will undergo optical microscope examination to view microstructures. SEM will be done to obtain information regarding the surface morphology of the electrospinning layer. Contact angle testing is a qualitative method for assessing the hydrophobicity or hydrophilicity of a surface. Contact angle testing is based on observing intermolecular interactions between the surface and water droplets when the water meets the surface. Contact angle testing is used to analyze the wettability and biocompatibility of magnesium samples before and after electrospinning.

The immersion test of pure magnesium samples with PVA/ZnAc electrospinning surface engineering was carried out using HBSS (Hank Balanced Salt Solution) solution referring to the ISO/FDIS 23317:2014 standard. The immersion test was carried out to evaluate ion release on samples that had been engineered with anodization and subjected to 3-point bending stress over a period of 28 days in the LUV – 101S model incubator (Figure 1). The immersion test follows the standard with a ratio of sample surface to solution volume of 0.1 ml/mm2. The manufacture of PVA/Zn nanofibers was carried out using electrospinning equipment with a static collector at a voltage of 13 kV, a flow rate of 0.1 mL/h, a distance between the needle tip and the collector of 12 cm, humidity of 50%, 23G syringe, and 5 syringe. ml. Electrospinning was carried out on magnesium miniplates attached to grounded aluminum foil.

Fig. 1. Incubator Machine Model LUV – 101S

3 Results & Dsicussion

Four variations of fiber layer samples, produced through electrospinning with different concentrations of ZnAc solution, were characterized for their chemical bonds using Fourier Transform Infrared Spectroscopy (FTIR). The FTIR spectrum was obtained in the range 4500 to 500 cm-1. The FTIR spectrum of PVA can be seen in the picture. Peaks A1, A2, A3, and A4 at 3400-3100 cm-1 indicate the presence of OH bonds. The existence of CH bonds is shown in peaks B1, B2, B3, and B4 at 2900-2800 cm-1. C=C bonds are shown at peaks C1, C2, C3, and C4 at 1560-1540 cm-1. Peaks D1, D2, D3, and D4 at 1420-1400 cm-1 indicate CO binding. Peaks E1, E2, E3, E4 at 1100-1000 cm-1 appear due to COC stretching. This shows that there is cross-linking between the -OH groups of PVA and ZnAc. Absorption peak at 620-600 cm-1 F1, F2, F3, F4 shows Zn-O bending. These peaks are in agreement with previous studies conducted on PVA/ZnAc electrospinning [23, 24].

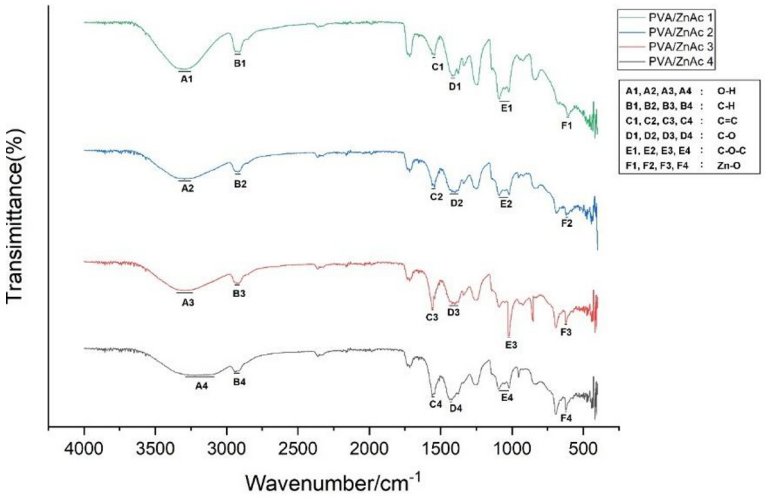

Fig. 2. FTIR spectrum of PVA/ZnAc

Results showed that the four magnesium samples coated with a layer of PVA/ZnAc electrospinning fiber have continuous fibers and do not have beads. The continuity and absence of beads in these four fiber layer samples is influenced by all electrospinning parameters, including process parameters, solution parameters and environmental parameters [25]. The morphology of the electrospinning fiber shows that the parameters used are optimum, namely a voltage of 13 kV, a flow rate of 0.1 mL/h, a distance between the needle tip and the collector of 12 cm, a humidity of 50%, a 23G syringe, and a 5 mL syringe. Changing one of the parameters greatly affects the morphology of the resulting fiber. Even though all variations of electrospinning fiber samples do not have beads, it can be seen in Figure 3(d) that with the highest ZnAc concentration, layers of beads or large droplets appear between the fiber layers and the fiber size is not homogeneous. This is caused by the instability of the electrospinning jet. A high ZnAc concentration affects the properties of the electrospinning solution such as viscosity, surface tension, and conductivity of the electrospinning solution. This will then affect the properties of the solution when it exits the jet to the collector [26].

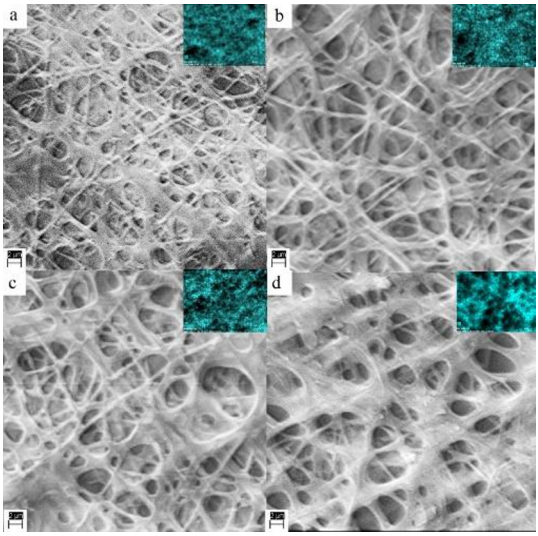

Fig. 3. Surface morphology of PVA/ZnAc Electrospinning Fiber Coating: (a) ZnAc 20%; (b) ZnAc25%; (c) ZnAc 33%; (d) ZnAc 50%

3.1 Fiber Diameter

Fiber diameter analysis also provides a comparison of the average fiber diameters of the four samples. The results of fiber diameter analysis show a trend of increasing fiber diameter along with increasing ZnAc concentration. In the PVA/ZnAc 1 sample, the average diameter value was obtained 0.1689 nm ± 0.07 nm which is shown in figure 4(a). Then the PVA/ZnAc 2 sample has an average diameter of 0.8743 nm ± 0.34 nm which is shown in figure 4(b). The next sample, namely the PVA/ZnAc 3 sample shown in Figure 4(c) has an average diameter of1,247 nm± 0.54 nm. PVA/ZnAc sample 4 has an average diameter2,162 nm± 0.86 nm.

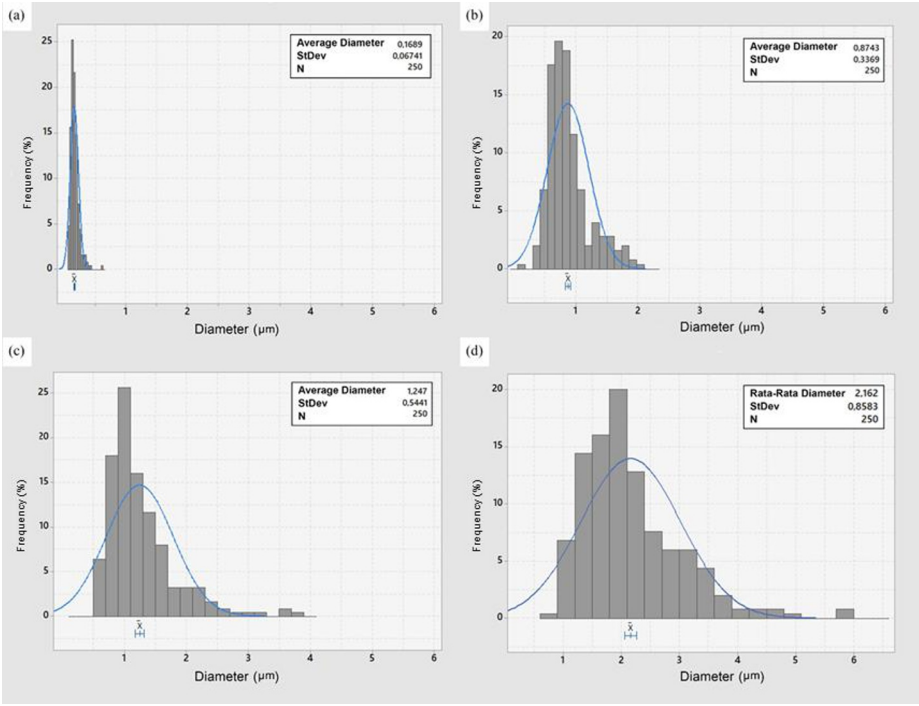

Fig. 4. Fiber Diameter Distribution HistogramElectrospinning PVA/ZnAc: (a) ZnAc 20%; (b) ZnAc 25%; (c) ZnAc 33%; (d) ZnAc 50%

It was found that the concentration of the ZnAc solution in the PVA/ZnAc solution mixture influenced the average diameter of the electrospinning fibers produced. The greater the concentration of the ZnAc solution in the electrospinning solution mixture, the greater the average fiber diameter produced in the fiber solution. Vice versa, the smaller the concentration of the ZnAc solution, the smaller the average fiber size produced [27, 28]. The relationship between solution concentration and fiber diameter can be seen in Figure 5. Changes in the average size of fiber diameter occur not only due to a single increase in solution concentration. However, the concentration of the solution will also change the viscosity and surface tension of the solution which will also affect the average size of the fiber diameter [29, 30].

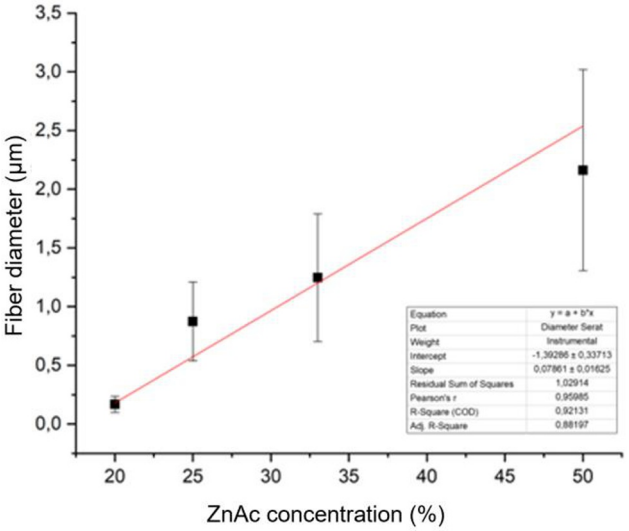

Fig. 5. Effect of ZnAc Solution Concentration on Fiber Diameter

3.2 Porosity Analysis

Porosity analysis was carried out using SEM images with a magnification of 3000 times which were processed using ImageJ softwareas shown in the picture. From the porosity analysis, it was found that the greater the concentration of the ZnAc solution, the greater the pore size and percentage of porosity of the PVA/ZnAc fiber layer. The results of the pore size analysis are clearly shown in Table 1. This is in accordance with the results of research conducted by. The trend of increasing porosity is shown in the figure 6-10.

Table 1. Porosity analysis results

Sample	Total Area (µm2)	Pore Area (µm2)	Porosity (%)
ZnAc 20%	8993.952	765,421	8.5%
ZnAc 25%	6602.5785	1471,959	22.3%
ZnAc 33%	6675.6382	2734.179	41.0%
ZnAc 50%	6748.7682	3208.293	47.5%

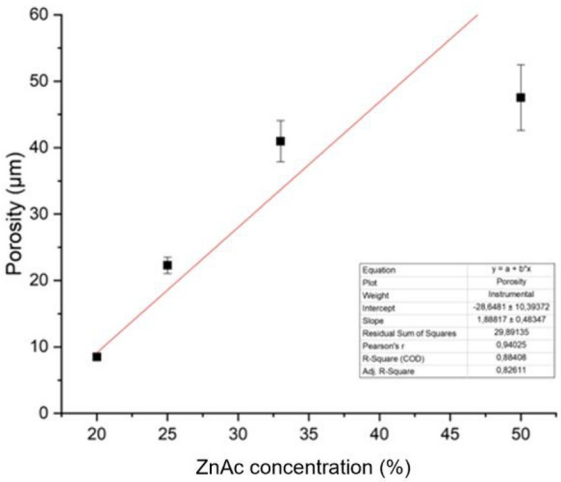

Fig. 6. Effect of concentration on porosity

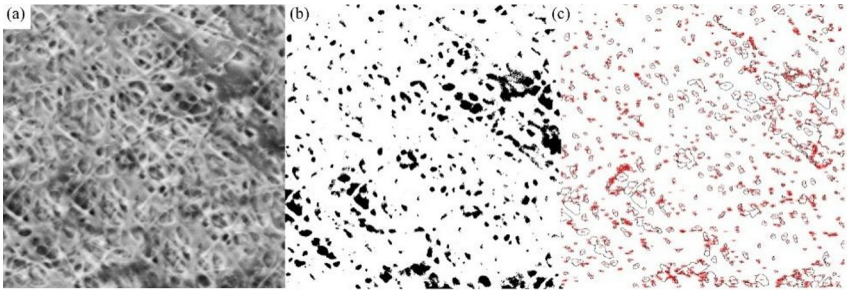

Fig. 7. Processing Process Porosity Analysis of 20% ZnAc Sample: (a) SEM Image; (b) Fig-Pore Threshold; (b) Pore Threshold Outline Image

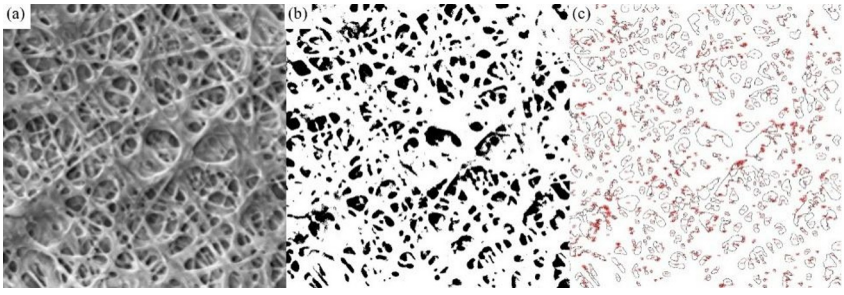

Fig. 8. Processing Process Porosity Analysis of 25% ZnAc Sample: (a) SEM Image; (b) Pore Threshold Image; (b) Pore Threshold Outline Image

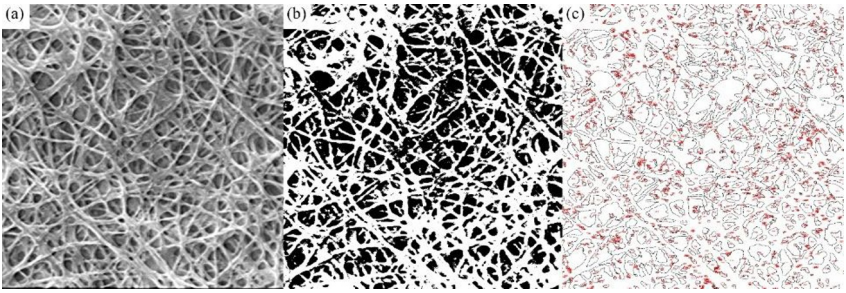

Fig. 9. Processing Process Porosity Analysis of ZnAc 33% Sample: (a) SEM Image; (b) Pore Threshold Image; (b) Pore Threshold Outline Image

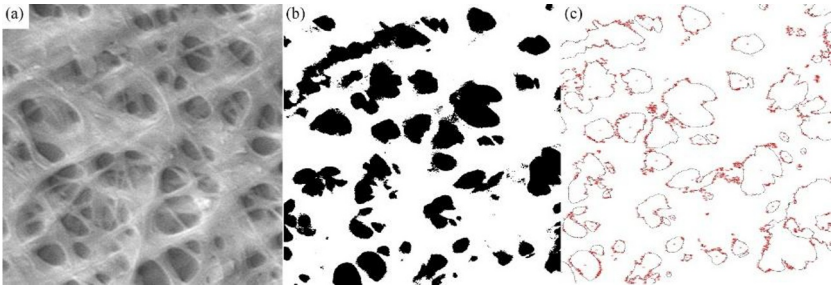

Fig. 10. Processing Process Porosity Analysis of 50% ZnAc Sample: (a) SEM Image; (b) Pore Threshold Image; (b) Pore Threshold Outline Image

3.3 Contact Angle Analysis

Contact angle analysis was carried out in this study with the aim of determining the wettability of each sample and to determine the relationship between wettability and solution concentration and fiber diameter. Testing was carried out at 5 random points using the drop test method, then the droplets were photographed with a camera and measurements were carried out using imageJ software. Figure 11(a) showed the first PVA/ZnAc sample obtained an average contact angle value of 44.76° ± 1.84°. The second sample (b) obtained an average contact angle value of 57.41° ± 3.75. PVA/ZnAc sample 3 (c) obtained an average contact angle value of 77.64° ± 5.2°. The fourth sample (d) obtained an average contact angle value of 83.33° ± 1.78°.

From the contact angle analysis carried out, a trend of increasing solution concentration was obtainedZnAc in the PVA/ZnAc electrospinning solution increases the hydrophobicity of the PVA/ZnAc fiber layer which can be seen in Figure 12 [31]. Increasing the solution concentration followed by increasing the fiber diameter increases the contact angle value. All samples are still in the hydrophilic category (<90°) even samples with a ZnAc concentration of 20% can be classified in the super hydrophilic category (<50°). The hydrophilic implant surface can improve the wound healing and osseointegration properties of the implant [32, 33].

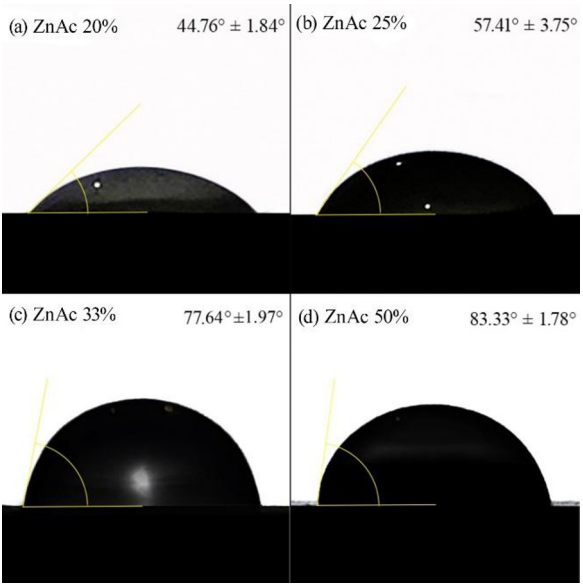

Fig. 11. Fiber Contact Angle MeasurementElectrospinning PVA/ZnAc : (a) 20% ZnAc; (b) 25% ZnAc; (c) 33% ZnAc; (d) 50% ZnAc

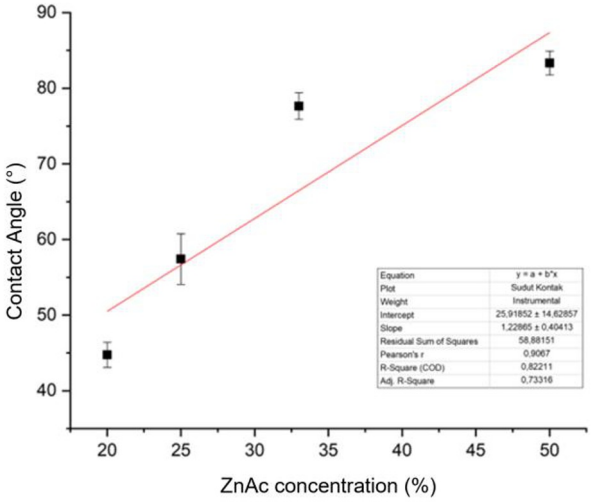

Fig. 12. Effect of Solution Concentration on Contact Angle

3.4 Immersion Test on Corrosion Rate

Immersion test analysis was carried out using weight loss tests and corrosion rate tests on magnesium implant samples. In the first and second weeks the weight loss test results and immersion test results showed that the corrosion rate and weight loss increased

along with increasing zinc acetate concentration. This is influenced by the size of the fiber diameter and porosity which increases with increasing zinc acetate concentration [34]. Increasing the fiber diameter and porosity will make it easier for the electrolyte to enter and interact with the Mg substrate so that the weight loss value and corrosion rate increase [35]. Then in the third- and fourth-weeks samples with zinc acetate concentrations of 33% and 25% experienced a significant increase in weight loss and corrosion rate. This can be caused by imperfect coating on the 33% zinc acetate and 25% zinc acetate coatings so that the coating easily separates from the Mg sample and corrodes significantly. In the 20% zinc acetate sample, the sample is coated on all sides thoroughly so that the layer formed is more thorough and can provide better corrosion protection. Then the good corrosion resistance of the 50% zinc acetate sample can be influenced by the highest concentration of zinc acetate among the other four samples. This is also stated by Vicente, et al [36]. Trends in weight loss and corrosion rate test results are shown in Figure 13-15 and table 2-3.

Table 2. Results of Weight Loss Test and Corrosion Rate Test for 7 and 14 Days

ZnAc concentration	Surface Area (mm2)	Initial Mass (mg)	Final Mass (mg)		Weight Loss (mg/mm2)		Corrosion Rate (mmy)	
			7 days	14 days	7 days	14 days	7 days	14 days
ZnAc 20%	395.46	435	0.432	0.428	0.008	0.018	0.002	0.003
ZnAc 25%	395.46	388	0.384	0.379	0.010	0.023	0.003	0.003
ZnAc 33%	144.92	290	0.286	0.28	0.028	0.069	0.008	0.010
ZnAc 50%	144.92	430	0.424	0.419	0.041	0.076	0.012	0.011

Table 3. Results of Weight Loss Test and Corrosion Rate Test for 21 and 28 Days

ZnAc concentration	Surface Area (mm2)	Initial Mass (mg)	Final Mass (mg)		Weight Loss (mg/mm2)		Corrosion Rate (mmy)	
			21 Days	28 Days	21 Days	28 Days	21 Days	28 Days
ZnAc 20%	395.46	435	0.423	0.415	0.030	0.051	0.003	0.004
ZnAc 25%	395.46	388	0.168	0.148	0.556	0.607	0.056	0.046
ZnAc 33%	144.92	290	0.14	0.272	1,035	1,242	0.104	0.093
ZnAc 50%	144.92	430	0.418	0.415	0.083	0.104	0.008	0.008

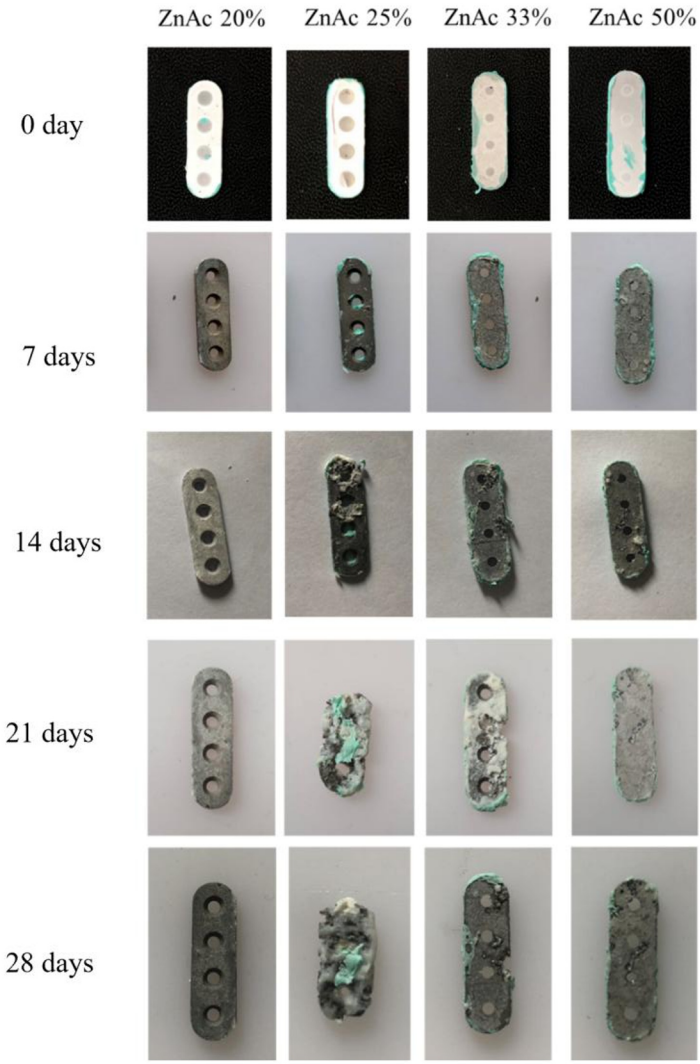

Fig. 13. Magnesium Implant Sample during the Immersion Test Process

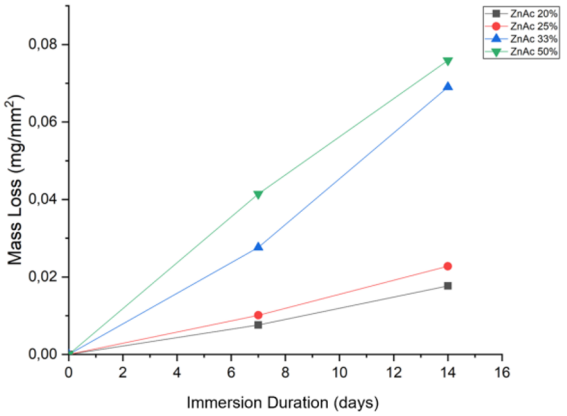

Fig. 14. Weight Loss after Immersion for 28 Days

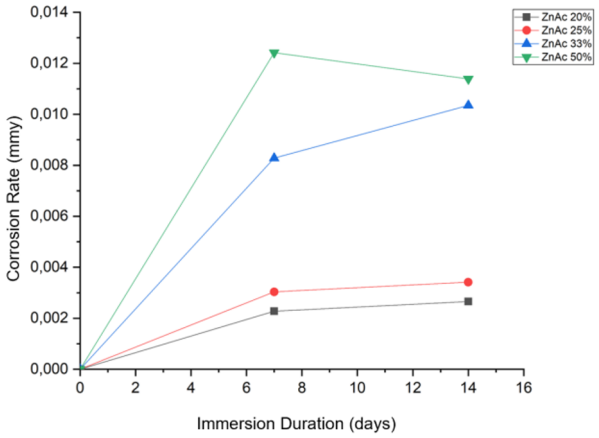

Fig. 15. Corrosion Rate Analysis Results after Immersion for 28 Days

4 Conclusion

These findings highlight several points, which are:

1. An increase in zinc acetate concentration within the PVA/ZnAc electrospinning solution leads to a noticeable enlargement in the average diameter of the resulting electrospun fibers.
2. Higher zinc acetate concentrations also contribute to the formation of thicker electrospun fiber layers on the magnesium implant surface.
3. The porosity of the electrospun fiber coatings increases in parallel with the zinc acetate concentration, potentially influencing the structural permeability of the layer.
4. As the zinc acetate content increases, the contact angle of the electrospun fibers also rises, indicating a trend toward more hydrophobic surface characteristics, although all samples remain within the hydrophilic range.

5. Elevated zinc acetate concentrations accelerate the corrosion rate of magnesium implants during the first and second weeks of immersion, primarily due to the increase in fiber diameter and porosity that facilitates electrolyte penetration. Moreover, a significant surge in corrosion was observed in samples with 25% and 33% zinc acetate during the third and fourth weeks, possibly attributed to incomplete or non-uniform coating coverage.

Acknowledgments. Authors would like to express sincere gratitude to Nanocenter, ILRC (Integrity Laboratory and Research Center), and TiBio, which provided the laboratory facilities and technical support necessary to carry out this research.

Disclosure of Interests. Authors declare no conflicts of interest.

Author Contributions. Conceptualization and Supervision, Sugeng and Bambang; methodology and research, Andi; writing—draft preparation and editing, Amirah. All authors have read and agreed to the published version of the manuscript.

Funding. This work was supported by "Seed Funding 2023 grant" from Faculty of Engineering, Universitas Indonesia (NKB-2569/UN2.F4.D/PPM.00.00/2023).

References

1. A. Hudecki, G. Kiryczyński, and M. J. Łos, "Chapter 7 - Biomaterials, Definition, Overview," in Stem Cells and Biomaterials for Regenerative Medicine, M. J. Łos, A. Hudecki, and E. Wiecheć Eds.: Academic Press, 2019, pp. 85-98.
2. P. Tong, Y. Sheng, R. Hou, M. Iqbal, L. Chen, and J. Li, "Recent progress on coatings of biomedical magnesium alloy," Smart Materials in Medicine, vol. 3, pp. 104-116, 2022/01/01/ 2022, doi: https://doi.org/10.1016/j.smaim.2021.12.007.
3. M. Saini, Y. Singh, P. Arora, V. Arora, and K. Jain, "Implant biomaterials: A comprehensive review," (in eng), World J Clin Cases, no. 2307-8960 (Print), 2015.
4. A. Abdal-hay, N. A. M. Barakat, and J. K. Lim, "Influence of electrospinning and dip-coating techniques on the degradation and cytocompatibility of Mg-based alloy," Colloids and Surfaces A: Physicochemical and Engineering Aspects, vol. 420, pp. 37-45, 2013/03/05/ 2013, doi: https://doi.org/10.1016/j.colsurfa.2012.12.009.
5. Z. Cai, P. Du, K. Li, L. Chen, and G. Xie, "A Review of the Development of Titanium-Based and Magnesium-Based Metallic Glasses in the Field of Biomedical Materials," Materials, vol. 17, no. 18, doi: 10.3390/ma17184587.
6. H. A. Zaman, S. Sharif, M. H. Idris, and A. Kamarudin, "Metallic Biomaterials for Medical Implant Applications: A Review," Applied Mechanics and Materials, vol. 735, pp. 19-25, 2015, doi: 10.4028/www.scientific.net/AMM.735.19.
7. M. B. Kannan, "13 - Biodegradable polymeric coatings for surface modification of magnesium-based biomaterials," in Surface Modification of Magnesium and its Alloys for Biomedical Applications, T. S. N. S. Narayanan, I.-S. Park, and M.-H. Lee Eds.: Woodhead Publishing, 2015, pp. 355-376.
8. M. P. Staiger, A. M. Pietak, J. Huadmai, and G. Dias, "Magnesium and its alloys as orthopedic biomaterials: A review," Biomaterials, vol. 27, no. 9, pp. 1728-1734, 2006/03/01/ 2006, doi: https://doi.org/10.1016/j.biomaterials.2005.10.003.

9. E. Müller et al., "The Biological Effects of Magnesium-Based Implants on the Skeleton and Their Clinical Implications in Orthopedic Trauma Surgery," Biomaterials Research, vol. 28, p. 0122, 2024, doi: 10.34133/bmr.0122.
10. L. Prawin Babu and R. Radha, "Advancements in magnesium-based alloys for orthopedic implants: balancing corrosion, mechanical properties, and biological effects (part 1) – a review," Canadian Metallurgical Quarterly, pp. 1-26, 2024, doi: 10.1080/00084433.2024.2427455.
11. A. Saberi et al., "A Comprehensive Review on Surface Modifications of Biodegradable Magnesium-Based Implant Alloy: Polymer Coatings Opportunities and Challenges," Coatings, vol. 11, no. 7, doi: 10.3390/coatings11070747.
12. A. Azizi Amirabad, M. Johari, R. Parichehr, R. Mehdinavaz Aghdam, C. Dehghanian, and S. R. Allahkaram, "Improving corrosion, antibacterial and biocompatibility properties of MAO-coated AZ31 magnesium alloy by Cu(II)-chitosan/PVA nanofibers post-treatment," Ceramics International, vol. 49, no. 11, Part A, pp. 17371-17382, 2023/06/01/ 2023, doi: https://doi.org/10.1016/j.ceramint.2023.02.106.
13. S. Vahedi, R. M. Aghdam, M. H. Sohi, and A. H. Rezayan, "Characteristics of electrospun chitosan/carbon nanotube coatings deposited on AZ31 magnesium alloy," Journal of Materials Science: Materials in Medicine, vol. 34, no. 1, p. 8, 2023/01/11 2023, doi: 10.1007/s10856-022-06703-1.
14. G. C. Türkoğlu, N. Khomarloo, E. Mohsenzadeh, D. N. Gospodinova, M. Neznakomova, and F. Salaün, "PVA-Based Electrospun Materials—A Promising Route to Designing Nanofiber Mats with Desired Morphological Shape—A Review," International Journal of Molecular Sciences, vol. 25, no. 3, doi: 10.3390/ijms25031668.
15. S. Ullah et al., "Stabilized nanofibers of polyvinyl alcohol (PVA) crosslinked by unique method for efficient removal of heavy metal ions," Journal of Water Process Engineering, vol. 33, p. 101111, 2020/02/01/ 2020, doi: https://doi.org/10.1016/j.jwpe.2019.101111.
16. R. Fatahian and R. Erfani, "Characterization and Optimization of Electrospun PVA/PLA Nanofibers Using Taguchi Method: Morphology and Structure," Journal of Electrostatics, vol. 134, p. 104035, 2025/03/01/ 2025, doi: https://doi.org/10.1016/j.elstat.2025.104035.
17. M. Koosha and H. Mirzadeh, "Electrospinning, mechanical properties, and cell behavior study of chitosan/PVA nanofibers," (in eng), J Biomed Mater Res A, no. 1552-4965 (Electronic), 2015.
18. D. Mailley, A. Hébraud, and G. Schlatter, "A Review on the Impact of Humidity during Electrospinning: From the Nanofiber Structure Engineering to the Applications," Macromolecular Materials and Engineering, vol. 306, no. 7, p. 2100115, 2021/07/01 2021, doi: https://doi.org/10.1002/mame.202100115.
19. R. M. Nezarati, E. Eifert Mb Fau - Cosgriff-Hernandez, and E. Cosgriff-Hernandez, "Effects of humidity and solution viscosity on electrospun fiber morphology," (in eng), Tissue Eng Part C Methods, no. 1937-3392 (Electronic), pp. 810-819, 2013.
20. P. K. Szewczyk and U. Stachewicz, "The impact of relative humidity on electrospun polymer fibers: From structural changes to fiber morphology," Advances in Colloid and Interface Science, vol. 286, p. 102315, 2020/12/01/ 2020, doi: https://doi.org/10.1016/j.cis.2020.102315.
21. A. Al-Abduljabbar and I. Farooq, "Electrospun Polymer Nanofibers: Processing, Properties, and Applications," Polymers, vol. 15, no. 1, doi: 10.3390/polym15010065.
22. M. Z. Zulkifli, D. Nordin, N. Shaari, and S. K. Kamarudin, "Overview of Electrospinning for Tissue Engineering Applications," Polymers, vol. 15, no. 11, doi: 10.3390/polym15112418.

23. M. Rosi, M. P. Ekaputra, M. Abdullah, and Khairurrijal, "Synthesis and Characterization of Cross-linked Polymer Electrolyte Membranes for Supercapacitor," AIP Conference Proceedings, vol. 1284, no. 1, pp. 55-58, 2010, doi: 10.1063/1.3515561.
24. S. Thakur, M. Kaur, W. F. Lim, and M. Lal, "Fabrication and characterization of electrospun ZnO nanofibers; antimicrobial assessment," Materials Letters, vol. 264, p. 127279, 2020/04/01/ 2020, doi: https://doi.org/10.1016/j.matlet.2019.127279.
25. M. L. A. Anero, A. D. S. Montallana, and M. R. Vasquez, "Fabrication of electrospun poly(vinyl alcohol) nanofibers loaded with zinc oxide particles," Results in Physics, vol. 25, p. 104223, 2021/06/01/ 2021, doi: https://doi.org/10.1016/j.rinp.2021.104223.
26. P. G. Ramos, N. J. Morales, R. J. Candal, M. Hojamberdiev, and J. Rodriguez, "Influence of zinc acetate content on the photoelectrochemical performance of zinc oxide nanostructures fabricated by electrospinning technique," Nanomaterials and Nanotechnology, vol. 6, p. 1847980416663679, 2016/01/01 2016, doi: 10.1177/1847980416663679.
27. T. Jamnongkan, S. Kaewpirom, A. Wattanakornsiri, and R. Mongkholrattanasit, "Effect of ZnO Concentration on the Diameter of Electrospun Fibers from Poly(Vinyl Alcohol) Composited with ZnO Nanoparticles," Key Engineering Materials, vol. 759, pp. 81-85, 2018, doi: 10.4028/www.scientific.net/KEM.759.81.
28. S. Rwei, R. Huang, and C.-C. Hung, "Electrospinning PVA Solution-Rheology and Morphology Analyses," Fibers and Polymers, vol. 13, p. 44, 01/01 2012, doi: 10.1007/s12221-012-0044-9.
29. E. Ghafari, Y. Feng, Y. Liu, I. Ferguson, and N. Lu, "Investigating process-structure relations of ZnO nanofiber via electrospinning method," Composites Part B: Engineering, vol. 116, pp. 40-45, 2017/05/01/ 2017, doi: https://doi.org/10.1016/j.compositesb.2017.02.026.
30. G. W. Peterson and T. H. Epps, "Impact of zinc salt counterion on poly(ethylene oxide) solution viscosity, conductivity, and ability to generate electrospun MOF/nanofiber composites," Polymer, vol. 252, p. 124816, 2022/06/14/ 2022, doi: https://doi.org/10.1016/j.polymer.2022.124816.
31. M. Khan et al., "Preparation and characterizations of multifunctional PVA/ZnO nanofibers composite membranes for surgical gown application," Journal of Materials Research and Technology, vol. 8, 11/01 2018, doi: 10.1016/j.jmrt.2018.08.013.
32. J. C. Ge, G. Wu, S. K. Yoon, M. S. Kim, and N. J. Choi, "Study on the Preparation and Lipophilic Properties of Polyvinyl Alcohol (PVA) Nanofiber Membranes via Green Electrospinning," Nanomaterials, vol. 11, no. 10, doi: 10.3390/nano11102514.
33. X. Yang, Y. Chen, C. Zhang, G. Duan, and S. Jiang, "Electrospun carbon nanofibers and their reinforced composites: Preparation, modification, applications, and perspectives," Composites Part B: Engineering, vol. 249, p. 110386, 2023/01/15/ 2023, doi: https://doi.org/10.1016/j.compositesb.2022.110386.
34. W. Ali, M. Echeverry-Rendón, A. Kopp, C. González, and J. Llorca, "Strength, corrosion resistance and cellular response of interfaces in bioresorbable poly-lactic acid/Mg fiber composites for orthopedic applications," Journal of the Mechanical Behavior of Biomedical Materials, vol. 123, p. 104781, 2021/11/01/ 2021, doi: https://doi.org/10.1016/j.jmbbm.2021.104781.
35. P. J. Rivero, D. M. Redin, and R. J. Rodríguez, "Electrospinning: A Powerful Tool to Improve the Corrosion Resistance of Metallic Surfaces Using Nanofibrous Coatings," Metals, vol. 10, no. 3, doi: 10.3390/met10030350.
36. A. Vicente, P. J. Rivero, J. F. Palacio, and R. Rodríguez, "The Role of the Fiber/Bead Hierarchical Microstructure on the Properties of PVDF Coatings Deposited by Electrospinning," Polymers, vol. 13, no. 3, doi: 10.3390/polym13030464.